

Available online at www.sciencedirect.com

jmr&t
Journal of Materials Research and Technology
journal homepage: www.elsevier.com/locate/jmrt



Original Article

Properties of sustainable self-compacting concrete containing activated jute fiber and waste mineral powders



Genbao Zhang^{a,d}, **Jiaqing Wang**^c, **Zhiwei Jiang**^e, **Cheng Peng**^e,
Junbo Sun^{b,*}, **Yufei Wang**^f, **Changfu Chen**^g, **Amr M. Morsy**^{h,i},
Xiangyu Wang^{f,**}

^a College of Civil Engineering, Hunan City University, Yiyang, Hunan 413000, PR China

^b Institute for Smart City of Chongqing University in Liyang, Chongqing University, Jiangsu, 213300, China

^c College of Civil Engineering, Nanjing Forestry University, Jiangsu 210037, PR China

^d Hunan Engineering Research Center of Structural Safety and Disaster Prevention for Urban Underground Infrastructure, Yiyang, Hunan 413000, PR China

^e School of Architectural Engineering, Nanjing Institute of Technology, Nanjing 211167, China

^f School of Design and Built Environment, Curtin University, WA 6102, Australia

^g College of Civil Engineering, Hunan University, Changsha, Hunan 410082, PR China

^h School of Architecture, Building and Civil Engineering, Loughborough University, Leicestershire LE11 3TU, United Kingdom

ⁱ Department of Civil Engineering, Cairo University, Giza 12613, Egypt

ARTICLE INFO

Article history:

Received 12 January 2022

Accepted 24 May 2022

Available online 30 May 2022

Keywords:

Ecological jute fibers

Waste mineral powders

Sustainable materials

Self-compacting concrete

Microstructures

ABSTRACT

Self-compacting concrete (SCC) mixtures requires a large amount of Portland cement and thus resulting in high CO₂ emissions, expanding its application has been in question to environment sustainability. Accordingly, environmental-friendly alternatives to Portland cement in SCC mixtures are deemed necessary for the progress of SCC in construction. In this investigation, treated jute fibers and mineral powders were used to replace cement in SCC mixtures. The effects of fibers and powder contents, fiber treatment, and mineral powder types on the workability and mechanical properties of SCC mixtures were investigated through slump-flow, compressive, and flexural tests. A microstructure was conducted through scanning electron microscopy. It was concluded that mineral powders and jute fibers could significantly improve the workability and mechanical properties of SCC. The microstructure observations demonstrated that the proposed methods are capable of enhancing the mechanical properties of SCC with an optimum fiber content. Specifically, a combination of 0.1% jute fibers and 75 μm zeolite powders were found to achieve the best mechanical properties. The relevant results supply fundamental reference and background for artificial intelligence and multi-function development for future infrastructure.

© 2022 The Authors. Published by Elsevier B.V. This is an open access article under the CC BY license (<http://creativecommons.org/licenses/by/4.0/>).

* Corresponding author.

** Corresponding author.

E-mail addresses: tunneltc@gmail.com (J. Sun), Xiangyu.Wang@curtin.edu.au (X. Wang).

<https://doi.org/10.1016/j.jmrt.2022.05.148>

2238-7854/© 2022 The Authors. Published by Elsevier B.V. This is an open access article under the CC BY license (<http://creativecommons.org/licenses/by/4.0/>).

1. Introduction

The use of cement for concrete production has risen to all-time maximum amid the significant increase in infrastructure development around the world, and especially in China. The manufacturing processes associated with the production of cement are primary contributors to the increase in CO₂ emissions and many other adverse impacts on the globe environment. Statistically, the production of Portland cement accounts for 5%–7% of the globe carbon dioxide emissions in 2013 [1]. In order to halt climate emergency, bringing net carbon dioxide emissions by the world economy to 0 is urgent because the any increase of carbon dioxide result in global warming [2]. In order to tackle these impacts, alternative materials and production methods are deemed necessary to minimize the environmental impacts while satisfying the growing infrastructure demands. Self-compacting concrete (SCC) has been extensively used in infrastructure construction to minimize the vibrations required to compact concrete, improve the mechanical properties of the concrete, and enhance the concrete workability and applicability [3,4]. However, large quantities of cementitious materials, particularly the Portland cement, are required for the production of SCC to achieve the high flowability with relatively higher water-cement ratios in comparison to those required for ordinary Portland cement concrete materials [5,6]. Therefore, expanding the use of SCC materials in construction would increase the use of Portland cement materials imposing an additional burden on the environment that limits the sustainable development of SCC materials [7]. In order to reduce the CO₂ emissions associated with the high demand of Portland cement in SCC production, pozzolans have been introduced as alternative cementitious materials in SCC mixtures [8–10]. In the meantime, disposal of mineral wastes imposes severe environmental threats as farmlands decrease, water pollution, and biodiversity damage due to increasing landfills [11,12]. To capitalize on the available resources of solid wastes from mining industry, mineral waste disposals have been increasingly used as pozzolans after appropriate processing and/or treatment [13,14]. Examples of mineral powders utilized as pozzolanic additives include zeolite [15], wollastonite [16] and binding Portlandite [17]. Thus, the utilization of waste mineral disposals (e.g., zeolite, wollastonite) as alternative cementitious materials could effectively reduce the use of Portland cements [18–20]. The effects of adding such waste pozzolan powders on the mechanical properties of SCC mixtures have not been well comprehensively investigated yet.

The performance of SCC depends not only on its workability during construction, but also on its load-carrying behavior in hardened stage [18,19,21]. Various fiber types were selected and introduced as reinforcement for SCC aiming to improve its tensile and flexural behaviors. Currently, the common fibers are mostly made from inorganic polymers. Even though these fibers have good ability in enhancing the mechanical performance of SCC, they are nondegradable materials that imposes adverse environmental impacts in the future [22–24]. Also, the production of inorganic polymers

generates CO₂ emissions that furtherly impacts the environment, energy consumption, and end-of-life treatment [25,26]. Recently, natural fibers have attracted attention as good alternatives to manufactured fibers for their biodegradability and low cost [27–29]. However, it has been reported that the inclusion of natural fibers in SCC could result in the loss of flowability, which was attributed to the increased fiber-binder frictional interaction [30], as well as the hydrophilic property of natural fibers in some cases. A couple of techniques including chemically alkali activation and physical vibration coating [31–33] were used to modify the surface properties of fiber to minimize the negative effect on flowability of SCC mixtures.

Jute fibers are easy to obtain with low energy demands and CO₂ emissions. They are considered one of the cheapest natural fibers that mainly contain cellulose and lignin [34–36]. Jute fibers have high strength and stiffness, and have recently been used as component for producing sustainable composite materials [19,37]. Therefore, the use of jute fibers in SCC could become an effective way for reinforcement. Nevertheless, the coupled effect of jute fibers and pozzolans on the mechanical properties of SCC has not been investigated. Also, the ingredient proportions of the additives have not been optimized to achieve the optimum performance of SCC. The rheological and mechanical performance optimization procedure should be conducted to investigate the feasibility of ecological jute fiber-reinforced SCC mixes with mineral additives [38–40].

The main contribution of this paper is the experimental investigation on the workability and mechanical properties of ecological jute fiber-reinforced SCC with waste mineral powders. Two types of pozzolans (zeolite and wollastonite) with different particle sizes were adopted in combination with a range of various fiber contents as testing variables. Three types of treatment methods were conducted on the jute fibers, i.e., free of treatment, alkali-activation, and ultrasonic vibration coating. The workability and mechanical performance of the prepared SCC mixtures were studied by slump-flow tests, compressive strength tests, and flexural strength tests. In addition, microstructural analysis was conducted on the jute fibers and prepared SCC specimens by using scanning electron microscope (SEM) to explore the mechanisms of fiber modifications and the effect of coupling jute fibers and pozzolans in the SCC specimens. The optimal proportion of reinforcement-pozzolan composition was proposed.

2. Experimental program

2.1. Preparation of materials

2.1.1. Selection of raw materials

The mixture of SCC was constituted of cement, fly ash, coarse aggregate, silica sand, water, superplasticizer, pozzolan and fiber reinforcement. The dosage of the above ingredients was specially calculated to ensure the manufacturability of SCC specimens used in the testing of their engineering properties [41].

Table 1 – Material properties of ingredients with consistent mixing fraction.

Ingredients Properties		Description	Value	
General Purpose Cement	Chemical Composition	CaO	63.40%	
		SiO ₂	20.10%	
		Al ₂ O ₃	4.60%	
		Fe ₂ O ₃	2.80%	
		SO ₃	2.70%	
		MgO	1.30%	
		Na ₂ O	0.60%	
		Total chloride	0.02%	
		CaO	63.40%	
		SiO ₂	20.10%	
	Physical Properties	Specific gravity	3000–3200 kg/m ³	
		Fineness index	390 m ² /kg	
		Normal consistency	27%	
		Setting time initial	120 min	
		Setting time final	210 min	
		Soundness	2 mm	
		Loss on ignition	3.80%	
		Residue 45-mm sieve	4.70%	
		Mechanical Properties	3-day compressive strength	38.6 MPa
			7-day compressive strength	48.4 MPa
28-day compressive strength	58.5 MPa			
28-day shrinkage	640 μm			
Fly Ash	Chemical Composition	SiO ₂	50.40%	
		Al ₂ O ₃	31.50%	
		Fe ₂ O ₃	10.40%	
		CaO	3.30%	
		TiO ₂	1.90%	
		MgO	1.10%	
		K ₂ O	0.50%	
		P ₂ O ₅	0.50%	
		Na ₂ O	0.30%	
		Mn ₂ O ₃	0.20%	
	SO ₃	0.10%		
	SrO	<0.1%		
	Physical Properties	Total alkali	0.60%	
		Relative density	2.29	
Moisture		<0.1%		
Loss on ignition		1.10%		
Silica Sand	Chemical Composition	SiO ₂	99.86%	
		Fe ₂ O ₃	0.01%	
		Al ₂ O ₃	0.02%	
		CaO	0.00%	
		MgO	0.00%	
		Na ₂ O	0.00%	
		K ₂ O	0.00%	
		TiO ₂	0.03%	
		MnO	<0.001%	
		Ignition Loss	0.01%	
	AFS Number	47.50%		
	Particle Size Distribution	Sieve size	Passing (%)	
		850 μm	0	
		600 μm	0.30	
425 μm		11.90		
300 μm	40.80			
212 μm	31.60			
150 μm	12.60			
106 μm	2.30			
75 μm	0.20			

Table 1 – (continued)

Ingredients Properties		Description	Value	
10-mm Natural Aggregate	Particle Size Distribution	Sieve size	Passing (%)	
		13 mm	100	
	Aggregate	9 mm	87	
		7 mm	20	
		4.75 mm	7	
		2.35 mm	4	
		1.18 mm	3	
		600 μm	2	
		300 μm	2	
		150 μm	2	
4-mm Natural Aggregate	Particle Size Distribution	Sieve size	Passing (%)	
		4.75 mm	100	
	Aggregate	2.36 mm	80	
		1.18 mm	55	
		600 μm	39	
		300 μm	27	
		150 μm	18	
		75 μm	13	
		Others	Apparent particle density	2.76 t/m ³
			Particle density dry	2.65 t/m ³
Particle density SSD	2.69 t/m ³			
Water absorption	1.40%			
Moisture content	2.50%			

P.O 42.5R Portland cement was used as the principal binder, while fly ash was added to improve the cohesion and reduce the heat of hydration. The pozzolan (wollastonite and zeolite) and aggregate were supplied by Fengtai Mineral Products Ltd., Hebei, China. The jute fiber was supplied by Xingyu Ltd., Anhui, China. Coarse-fine aggregates were prepared by utilizing natural aggregates and silica sands. The superplasticizer was specially employed to attain better fluidity under dispersion effect and appropriate water usage. The properties of all selected materials are summarized and presented in Table 1.

2.1.2. Treatment of jute fibers

The jute fibers were pre-treated before mixing into SCC mixtures with three different treatment techniques, i.e., the free-of-treatment (FOT), the alkali activation treatment (AAT), and the ultrasonic vibration coating treatment (UVCT), respectively. The AAT was implemented by keeping jute fiber specimens soaked in NaOH solute (1 percent concentration) for 20 min and air dried in ambient temperature. The UVCT was carried out using an intelligent ultrasonic processor (Buena Biotech, BEM-650A). A nano-size silica sand was adopted as wrapping agent to form the fiber coating under a 0.9 percent mass ratio of jute fiber specimen during the UVCT process [42]. The physical specification of nano-size silica sand is presented in Table 2.

2.2. Mixture design

In this investigation, the content of pozzolan and fiber were adopted as testing variables in mixing of SCC by changing mineral powder type and size, as well as changing pre-treatment method and mixing proportion for fibers. All other materials were kept consistent through all specimen

types. The zeolite and wollastonite powders were used as pozzolan materials because they possess active silica dioxide and aluminum oxide, which contribute to the mechanical strength of SCC. Meanwhile, the utilization of zeolite and wollastonite powders, as waste mineral powders, is beneficial to sustainability when they replace cement. To seek the feasibility of waste mineral powders to replace cement, the nominal particle size of utilized zeolite and wollastonite is chosen as 75 μm , which is similar to that of cement. Besides, the main purpose of 300 μm nominal particle size is to distinctly compare the size effect of both zeolite and Wollastonite on the rheological and mechanical properties of SCC. Therefore, two different nominal particle size of 75 and 300 μm was prepared for both types of powders, respectively. Specifically, the four types of pozzolan specimens (denoted by zeolite-75, zeolite-300, Wollastonite-75, and Wollastonite-300) were characterized by laser particle size analyzer and the respective particle size distribution curves are presented in Fig. 1.

As mentioned above, four testing variables, i.e., the type of pozzolan, the size of pozzolan, the type of treatment method for jute fiber, and the content of jute fiber, were adopted in the testing program. For the purpose of deriving the respective impact of each testing variable, the variance of testing variables was represented by different levels, as specified in Table 3. A comprehensive design was used for different levels of testing variables to implement the testing scheme, which results in a total of 48 combinations of testing variables as presented in Table 4. It is noted that the type and content of remaining ingredients in mixing other than pozzolan and fiber were consistent throughout the testing program, except the control group where pozzolans and fibers were not introduced into the mixture.

2.3. Testing procedure

2.3.1. Preparation of specimens

The SCC specimens were prepared corresponding to the testing variable combinations shown in Table 3 according to the testing specifications AS1012.9 [43]. It is noted that three parallel specimens, in different dimensions according to respective testing protocols, were manufactured for every single variable combination, which was used in uniaxial compressive strength test, flexural strength test, and slump flow test, respectively [25,44,45]. The demolding time, in this case, is 48 h instead of 24 h to reduce the demolding effect on the samples and guarantee strength development of SCC specimens. It is noted that the 48-h demolding time is set for all samples to ensure there is no influence on the final results' comparison. After demolding, the specimens were cured in the curing room at 20 ± 2 °C with 95% humidity.

2.3.2. Slump flow test

The fresh properties (flowability, viscosity, and passing ability) of SCC specimens were tested using slump flow experiment and J-ring analysis as per specifications [46]. Abrams cone was employed in the listed experiments complying with AS1012.14 [47].

2.3.3. Uniaxial compressive strength test

The SCC specimens in the compressive strength test were $50 \times 50 \times 50$ mm in dimension and cured until the testing date. All the mechanical test procedures are finished by BLH (Baldwin Lima–Hamilton) pressure testing machine in accordance with AS1012.14 [47] and AS1012.9 [43] with a 0.2 kN/s loading rate. The elastic modulus of concrete can be measured simultaneously with the utilization of vertical strain gauges.

2.3.4. Flexural strength test

The flexural strength of the SCC specimens was tested, complying with the protocol given in ASTM C348 [48]. The SCC specimens used in the flexural strength test were $40 \times 40 \times 160$ mm in dimension and loaded with a loading rate of 0.03 MPa/s until the testing date.

2.3.5. Statistical analysis of strength development

The mechanical performance of SCC was evaluated by testing the flexural and compressive strengths at 7-day, 14-day, and 28-day curing durations. Aiming to demonstrate the modifying effect of introducing reinforcements and pozzolans, the normalized strength, i.e., the strength ratio of the specimen of interest and the specimen in the control group, was used, as exemplified in Fig. 2. The comparative details of modifying efficiency in terms of flexural strength can be more readily observed using normalized strengths than that using absolute strengths. In fact, the strength enhancement reaches the peak in 14-day curing duration while the absolute strength grows all the way through the increasing curing time for all specimens without fiber inclusions except for the ones introducing 75 μm -zeolite pozzolans. Hence, the normalized flexural and compressive strengths (NFS and NCS) were consistently used throughout the results and discussions without giving special notes.

2.3.6. Variable significance for mechanical performance

An approach based on sensitivity analysis (SA) was used to investigate the relationship between variables and output results. Within the value range of input variables, this method can assess the impact on the output by changing the input values [49]. The beginning procedure is to design input and output variables, followed by evaluating each input variable with all the other variables constant. This study applies the global sensitivity analysis (GSA) and the importance sequences (0–100%) are visualised [50]. The following equations show a gradient metric to estimate the resulting change of the output and the relative importance formulation [50].

Table 2 – Physical specifications for nano-size silica sand.

Properties	Value
Purity (wt%)	99.7
Average Size (nm)	500
Ignition Loss (wt%)	4.8
Dibutyl Phthalate Absorption Value (ml/g)	3.6

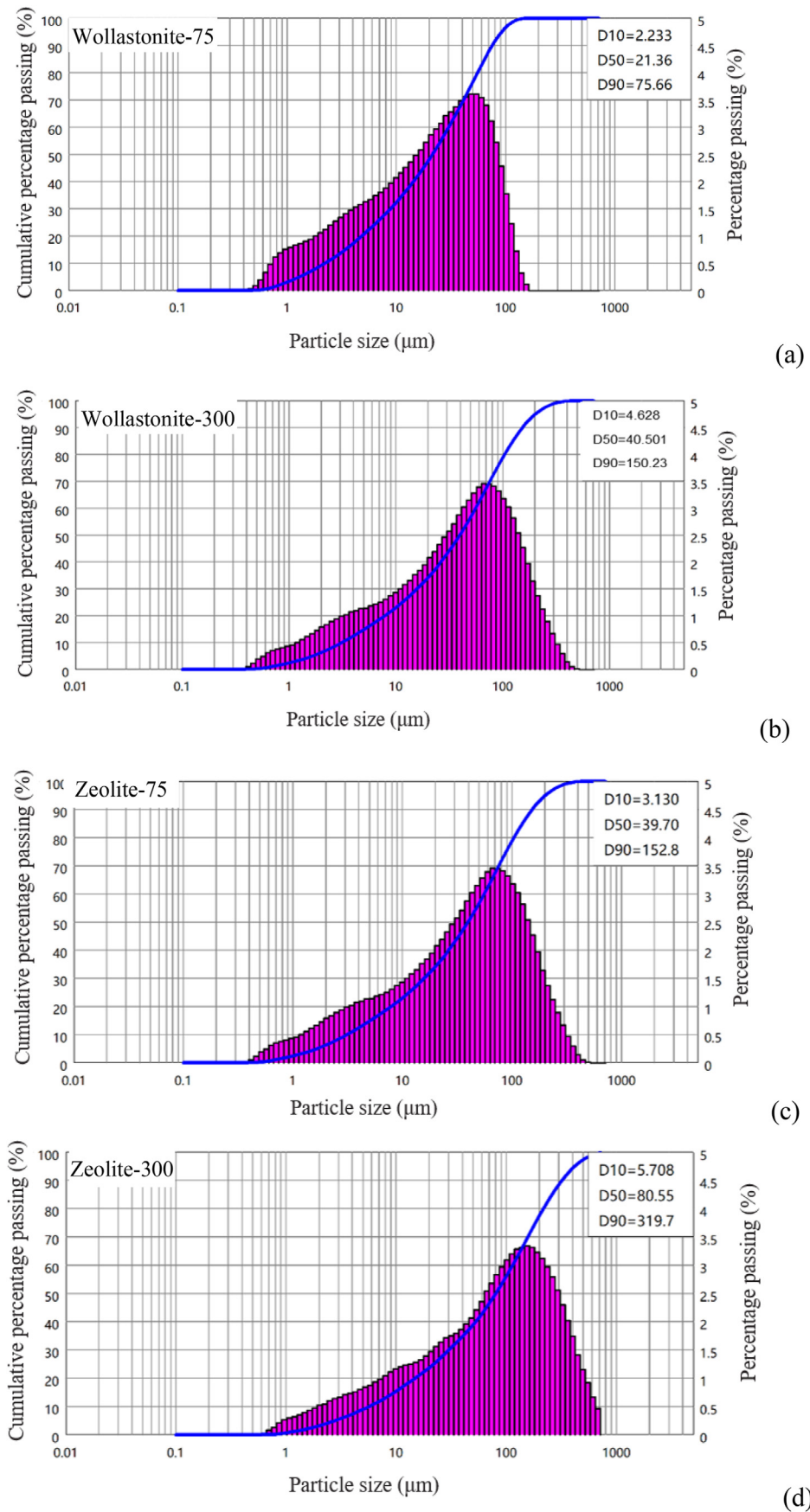


Fig. 1 – Particle size distribution curves for (a) Wollastonite-75, (b) wollastonite-300, (c) zeolite-75 and (d) zeolite-300.

Table 3 – Testing variables and respective levels in the testing program.

Testing variables	Levels
The type of pozzolan	zeolite; Wollastonite
The size of pozzolan	75 mm; 300 mm
The type of fibre treatment	FOT; AAT; UVCT
The volumetric content of jute fibre	0; 1%; 2%; 3%
The replacement volume of binder	15%

$$g_{\varepsilon} = \sum_{j=2}^L \frac{|\widehat{y}_{\varepsilon,j} - \widehat{y}_{\varepsilon,j-1}|}{L - 1} \tag{1}$$

$$R_{\varepsilon} = g_{\varepsilon} / \sum_{i=1}^I g_i \tag{2}$$

where ε is the analysed input variable; $\widehat{y}_{\varepsilon,j}$ represents the susceptibility reaction indicator for $x_{\varepsilon,j}$; R_{ε} is the relative importance of the variable.

Table 4 – Testing scheme with ingredient proportion of the mixture per unit volume (m³).

ID	Pozzolan	Size (µm)	Fibre treatment	Fibre mass (kg)	Fibre Vol (%)	Cement mass (kg)	Fly ash mass (kg)	Pozzolan mass (kg)	Aggregate mass (kg)	Silica sand (kg)
Control	NA			0		280	220	0		
Z075F00	Zeolite	75	FOT	0	0					
Z075F10				1.45	1					
Z075F20				2.9	2					
Z075F30				4.35	3					
Z075A00			AAT	0	0					
Z075A10				1.45	1					
Z075A20				2.9	2					
Z075A30				4.35	3					
Z075U00			UVCT	0	0	238	187	75	400	200
Z075U10				1.45	1					
Z075U20				2.9	2					
Z075U30				4.35	3					
Z300F00		300	FOT	0	0					
Z300F10				1.45	1					
Z300F20				2.9	2					
Z300F30				4.35	3					
Z300A00			AAT	0	0					
Z300A10				1.45	1					
Z300A20				2.9	2					
Z300A30				4.35	3					
Z300U00			UVCT	0	0					
Z300U10				1.45	10					
Z300U20				2.9	20					
Z300U30				4.35	30					
W075F00	Wollastonite	75	FOT	0	0					
W075F10				1.45	10					
W075F20				2.9	20					
W075F30				4.35	30					
W075A00			AAT	0	0					
W075A10				1.45	10					
W075A20				2.9	20					
W075A30				4.35	30					
W075U00			UVCT	0	0					
W075U10				1.45	10					
W075U20				2.9	20					
W075U30				4.35	30					
W300F00		300	FOT	0	0					
W300F10				1.45	10					
W300F20				2.9	20					
W300F30				4.35	30					
W300A00			AAT	0	0					
W300A10				1.45	10					
W300A20				2.9	20					
W300A30				4.35	30					
W300U00			UVCT	0	0					
W300U10				1.45	10					
W300U20				2.9	20					
W300U30				4.35	30					

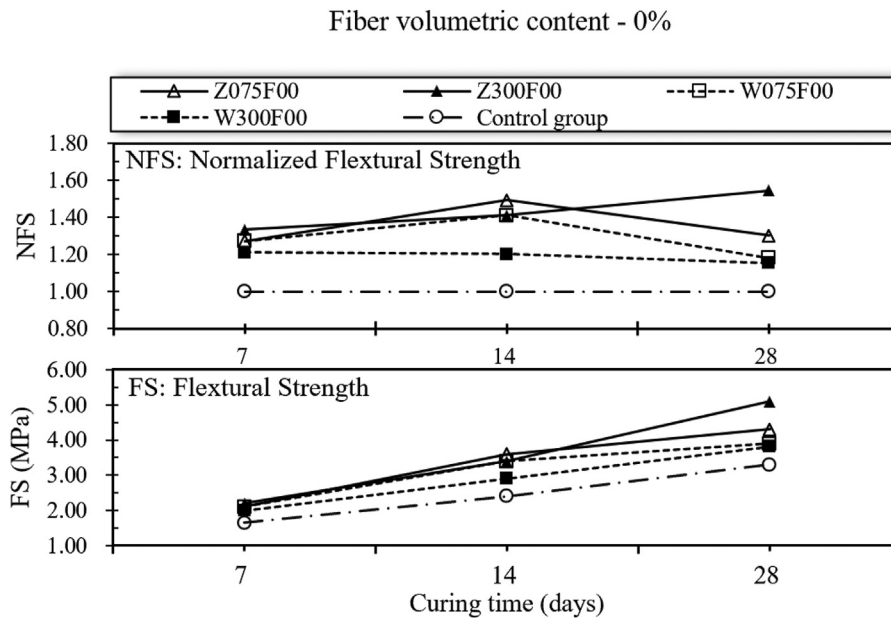


Fig. 2 – The explanation of the relationship between flexural strength (FS) and normalized flexural strength (NFS).

2.3.7. Microstructural visualization

Scanning electron microscopy (SEM) was employed to visualize the microstructural evolution of specimens by introducing different pozzolans, jute fibers. The failure SCC specimens after the flexural strength test were also collected to be observed by the SEM.

3. Results and discussion

3.1. Fresh property

The fresh property (flowability) of fresh SCC mixtures were evaluated based on the slump flow test, the results are shown in Figs. 3–10. In order to clearly compare the results, the slump flow measurements were divided into three groups in

terms of the different fiber treatment methods. The slump flow diameter of control group without the addition of jute fiber and mineral powders was 650 mm. Regarding to the specimens without any fiber modification, the slump flow and J-ring diameter were in ranges from 490 to 700 mm and from 385 to 575 mm, as shown in Fig. 3 and Fig. 4, respectively. The slump flow and J-ring diameter reduced with the increased fiber content as shown in Z075-F, Z300-F, and W300-F mixtures. However, the W075-F mixture represented distinct behavior. When the fiber content increased from 0.1% to 0.2%, the slump flow and J-ring diameter increased instead of decreasing, which may attribute to lubrication effect of wollastonite powder with the optimum size of 75 μm. Thereafter, the further increase of fiber content reduced the slump flow and J-ring diameter since the agglomeration and larger

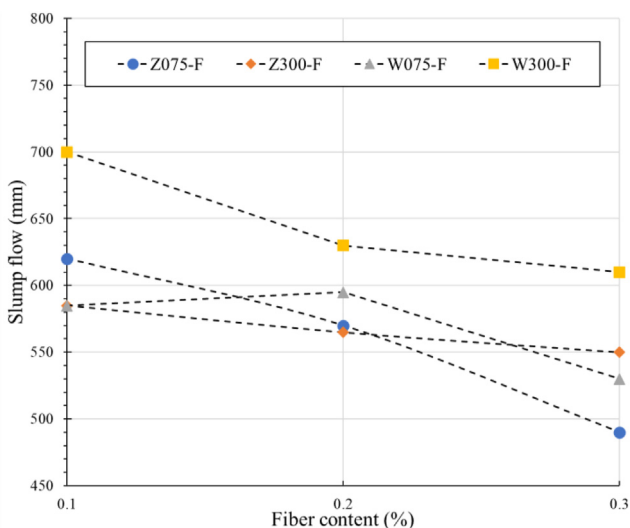


Fig. 3 – The slump flow test results of specimens without fiber treatment.

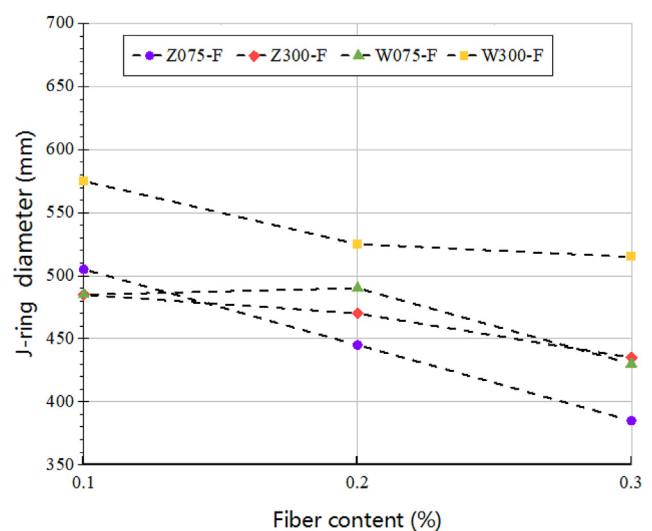


Fig. 4 – The J-ring test results of specimens without fiber treatment.

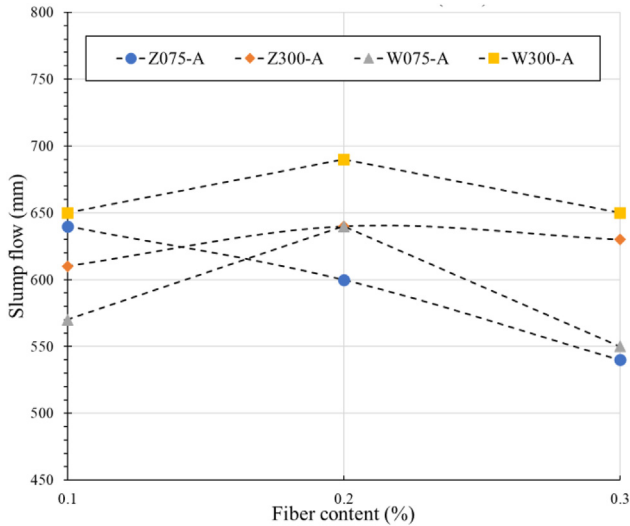


Fig. 5 – The slump flow test results of specimens with AAT fiber treatment.

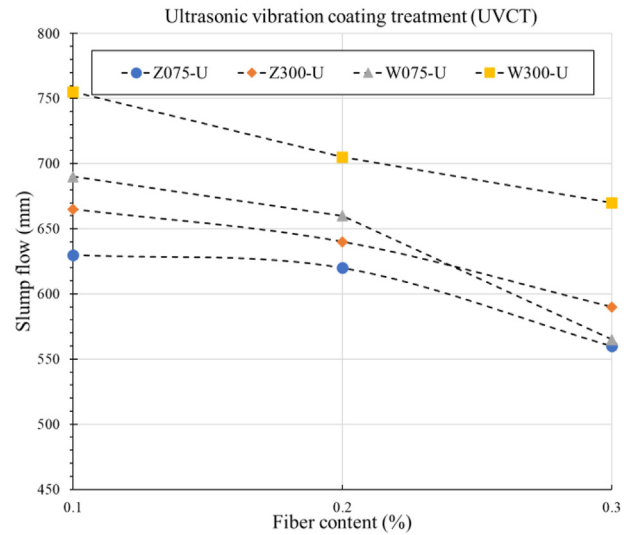


Fig. 8 – The slump flow test results of specimens with UVCT fiber treatment.

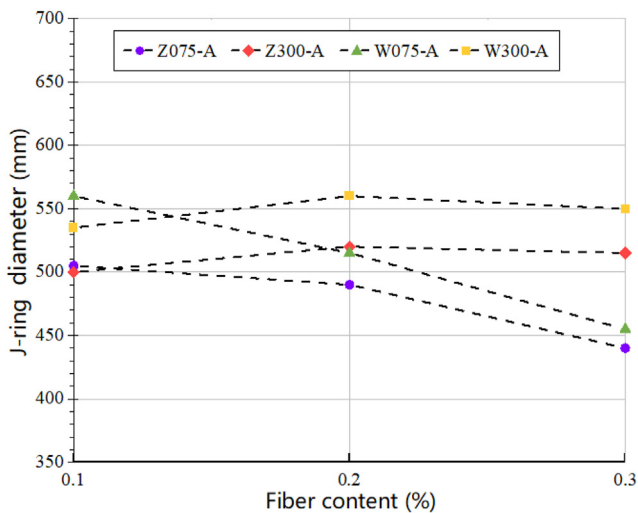


Fig. 6 – The J-ring test results of specimens with AAT fiber treatment.

friction inside of the mixture with more fibers. The increase of wollastonite powder size from 75 to 300 μm also increased the slump flow because of the smaller particles may lead to a

better compaction of the mixture with reduced air voids content, thus improving the flowability of the fresh mixture. When considering the different pozzolan types, the introduction of wollastonite resulted in a higher slump flow and J-ring diameter by comparing with the addition of zeolite. The porous structure of zeolite could absorb cement paste during the mixing process, and finally reduce the free cement paste in the fresh mixture that dominates the flowability.

The slump flow and J-ring diameter results of AAT modified jute fiber reinforced SCC mixtures are illustrated in Fig. 5 and Fig. 6, respectively. The slump flow and J-ring diameter were in respective ranges from 530 to 690 mm and from 440 to 560 mm. After the AAT treatment, the trends of slump flow and J-ring diameter change with the increase of fiber content. The slump flow of all mixture was increased when the fiber content was increased from 0.1% to 0.2%, except the Z075-A mixture. In general, the flowability was improved with the AAT treatment in most of mixtures when compared with that of free-of-treatment mixtures, as shown in Fig. 7. The AAT treatment changed the surface microstructures of jute fiber, which may contribute to the elimination of agglomeration. The pozzolan types effect was still consistent in the AAT modified mixtures with the free-of-treatment mixtures.

The slump flow and J-ring diameter of mixtures with UVCT modified jute fiber is represented in Figs. 8 and 9, respectively.

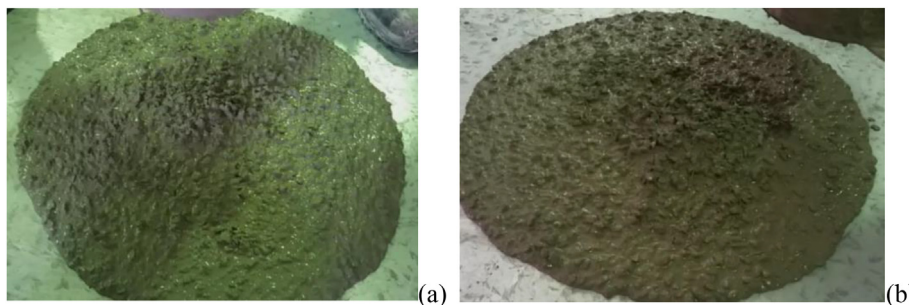


Fig. 7 – Slump experiment for SCC mixes with (a) 0.3% jute fiber and (b) 0.3% AAT treated jute fiber.

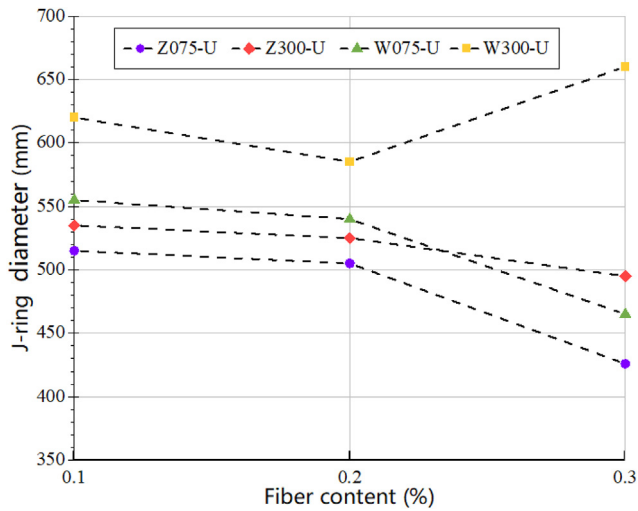


Fig. 9 – The J-ring test results of specimens with UVCT fiber treatment.

The slump flow and J-ring diameter were in respective ranges from 560 to 755 mm and from 425 to 660 mm. It can be noted that the slump flow and J-ring diameters were significantly increased after the UVCT modification when compared with the previous results of other two types of treatment methods, as demonstrated in Fig. 10. Therefore, the UVCT methods could effectively increase the flowability of SCC mixture with the addition of jute fiber and pozzolans, which may be attributed to the smooth coating layer on fiber surface after the UVCT modification, which dramatically eliminates the agglomeration of jute fibers.

3.2. Three-point flexural strength

The NFSs of SCC specimens are presented respectively in Figs. 11–14 corresponding to SCC specimen groups mixed by four types of pozzolans, i.e., Z075, Z300, W075 and W300. The variance of NFS over the increasing fiber volumetric content was depicted in three subfigures in each group corresponding to three types of fiber treatment methods: (i) the FOT; (ii) the AAT; and (iii) the UVCT with abbreviations of F, A and U, respectively.

As shown in Fig. 11, the flexural strength enhancement evolves distinctly over the increase of fiber content for Z075 specimens using different fiber treatment methods. It is noteworthy that the NFS of Z075-F specimens without fiber treatment decreases with the increasing fiber content during all curing times. Without the fiber treatment, the bond between the jute fiber and cement matrix is weak. Thus, the integrity of the entire matrix could be affected. At the same time, the increased fiber content may result in more air voids content, and finally reduces the flexural strength [51]. It is observed that the NFSs of specimens at all curing times drops to the under-unit zone as indicated by grey block when the fiber volumetric content increased to 3%. This illustrates that the introduction of 3% jute fiber might impair the strength development rather than enhance the SCC specimens. However, the peak of strength enhancement can be observed for Z075-A and Z075-U specimens with increased fiber content. The peaks were consistently observed for all curing times at fiber content of 0.1% in Z075-A, while the peak switches from 0.1% fiber content in 7-day curing time to 0.2% fiber content in 14-day and 28-day curing times in Z075-U. When comparing the two different treatment methods, the specimens with UVCT-treated jute fiber achieved a higher strength than that of AAT-treated jute fiber in terms of a higher fiber addition

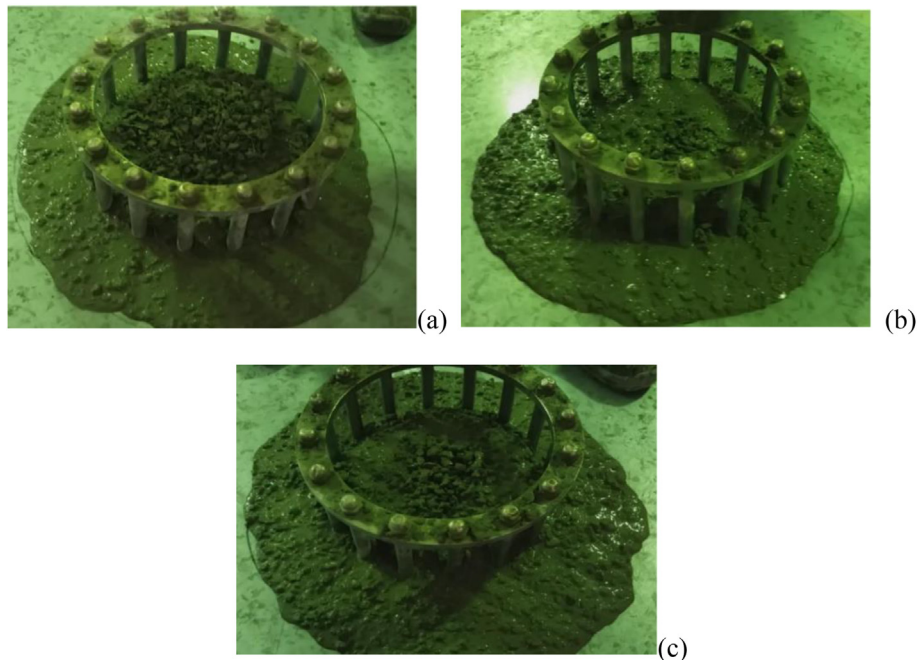


Fig. 10 – J-ring test for SCC mixes with (a) 0.3% jute fiber, (b) 0.3% AAT treated jute fiber, (c) 0.3% UVCT treated jute fiber.

content. The above observations indicate that the fiber treatment of Z075 specimen is able to improve the FS enhancement within a limited fiber content. Therefore, after the AAT treatment method, the jute fiber presented a modified surface microstructure, which may help to improve the mechanical bond between the treated fiber and cement matrix. At the same time, the UVCT treatment method with nano-sized silica coating layer on the jute fiber could furtherly improve the bonding strength between jute fiber and cement matrix. The silica layer could participate the chemical reactions through the cement hydration processes [52].

With respect to Z300 specimens shown in Fig. 12, the increase of fiber content can lead to the improved FS enhancement as shown in the UVCT specimens. However, the different trend was observed in FOT and AAT specimens, in which the NFS is reduced with the increased fiber content. In subfigures Z300-F and Z300-A, the most effective strength enhancement was observed in Z300 specimens without introducing fibers. Similar to the observations in Fig. 11, the improvement of FS enhancement induced by fiber content increase is limited within a range under 0.2% fiber content where the peak of NFS were observed for all curing times (see in subfigure Z300-U). Therefore, the change of zeolite size could also affect the effectiveness of the fiber reinforcement. The proper size of mineral powders should be considered to achieve the optimum flexural strength enhancement [53].

In addition, the comparison of the mineral powder types with the same particle sizes are conducted. The results of transition of pozzolan type from zeolite to wollastonite under the same size (Z075 to W075) are shown in Fig. 13. In this figure it can be observed that more obvious FS enhancement with increased fiber content by comparing with that of Z075 specimens. The enhancement peak can be found at 0.1% fiber content for specimens without fiber treatment (see subfigure W075-F), which is not the case in subfigure Z075-F. The consistently developed increase of NFS over fiber content increase were observed for all curing times in W075-A, which implies that the AAT of fiber can ensure the content-increase-induced FS enhancement within a larger content range for W075 fibers. On contrast, the UVCT of fiber can merely ensure the improved FS enhancement within a range under 0.2% fiber content (see subfigure W075-U).

The size effect of wollastonite (W075 to W300) on the improvement of FS enhancement over increasing fiber content can obviously observed in Fig. 14. The consistent improvement can be found in subfigure W300-F, and overall improvement found in subfigure W300-U except for slight increase observed in 0.1 fiber content for 7- and 14-day curing times. The peak of improved FS enhancement appears at 0.1 fiber content for W300-A specimens (see subfigure W300-A), which reveals that the AAT of fiber failed to extend the improvement of FS enhancement to a larger fiber content.

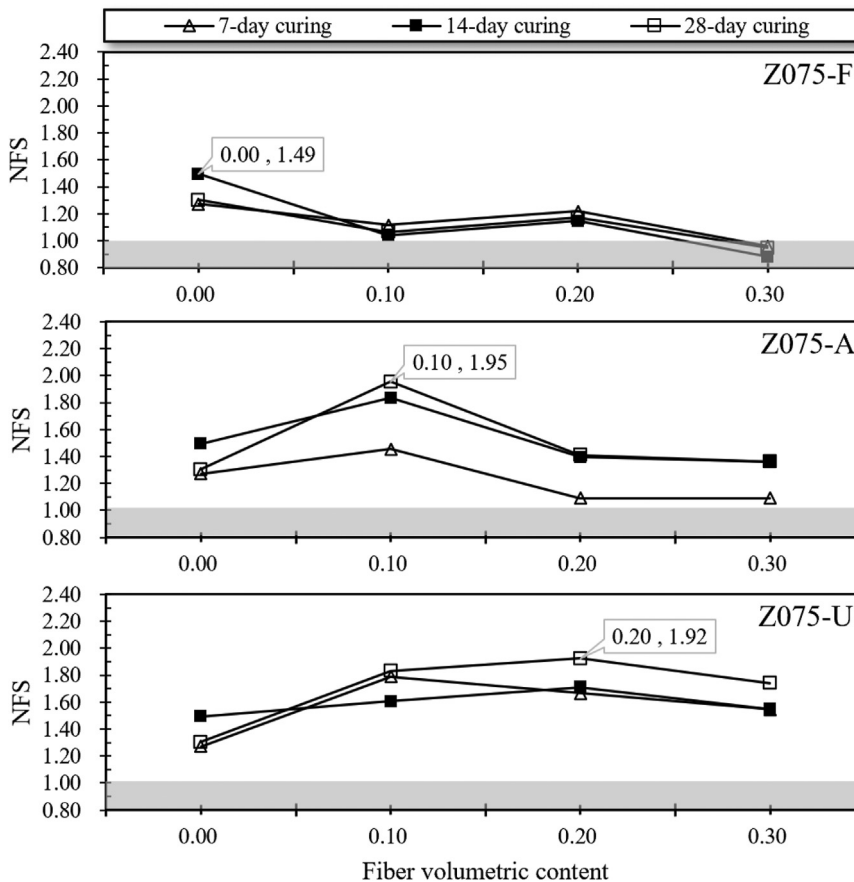


Fig. 11 – Flexural strength enhancement for Z075 group.

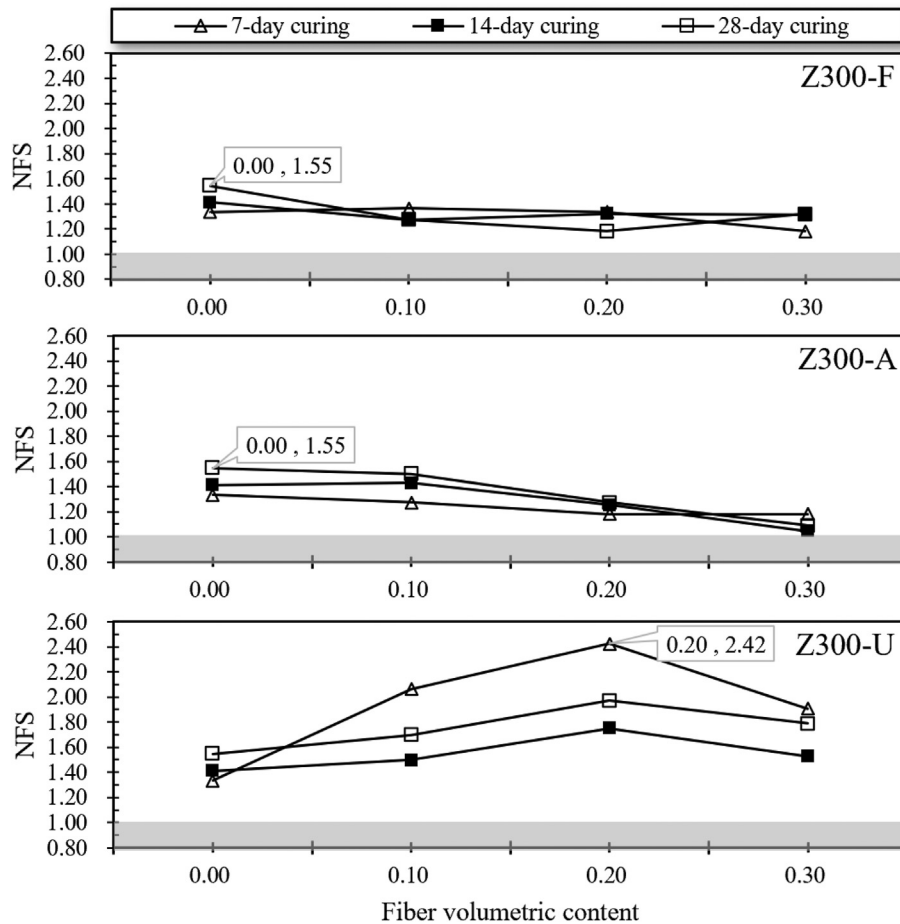


Fig. 12 – Flexural strength enhancement for Z300 group.

3.3. Uniaxial compressive strength

The compressive behavior of modified SCC specimens was specially evaluated in conjunction with the flexural behavior by testing the uniaxial compressive strength (CS) since it is reported that the inclusion of fibers tends to undermine the compressive resistance by introducing more fiber-binder interfaces [39,54]. The evolution of NCS enhancement against the increase of fiber volumetric content was particularly concerned in evaluating the NFS, which renders a focus on the modifying effectiveness of reinforcement on the SCC specimens with certain pozzolans under certain curing time.

For specimens with Z075 pozzolans, the NCS enhancement can be improved monotonically by mixing increasing fibers into the binders. This improving fashion is independent of curing times, when the fibers were subjected to AAT, as shown by Z075-A columns in Fig. 15. It is noted that the change of NCS enhancement for specimens with varying fiber contents is insignificant if the fiber is free of surface treatment (FOT) over the increasing curing times.

When Z300 pozzolans were mixed in SCC specimens, the same combinations of fiber content and treatment method can be found for the maximum NCS enhancement under 14-day and 28-day curing time, i.e., the combination of 0.1%

fiber volumetric content and fiber treatment of UVCT (see Fig. 16). The UVCT treatment for fibers in Z300 specimens can result in better NCS enhancement than other treatment methods for most of fiber contents. However, the most outstanding performance of NCS enhancement for Z300 specimens is induced by the combination of 0.2% fiber content and AAT fiber treatment at 7-day curing time. It indicates that the AAT could expedite dramatically the strength growing progress of Z300 specimens, leading to a competitive enhancement behavior of early compressive strength [55,56].

It is noteworthy that the NCS enhancement for specimens with the pozzolan, W075 and W300, displayed a very consistent combination of fiber content for excelled performance, i.e., the maximum NSC at fiber volumetric content of 0.1%, as seen in Figs. 17 and 18. The above trend of fiber content is independent of the curing time and pozzolan size, but the treatment method inducing the maximum NCS is influenced by the curing time. For early curing time (7-day), the combination of the maximum NCS is induced by the absence of treatment (FOT), while for the remaining curing times (14- and 28-day), the combination of the maximum NCS is consistently accompanied by UVCT. It reveals that the UVCT is necessarily required to provide the most prominent NCS enhancement

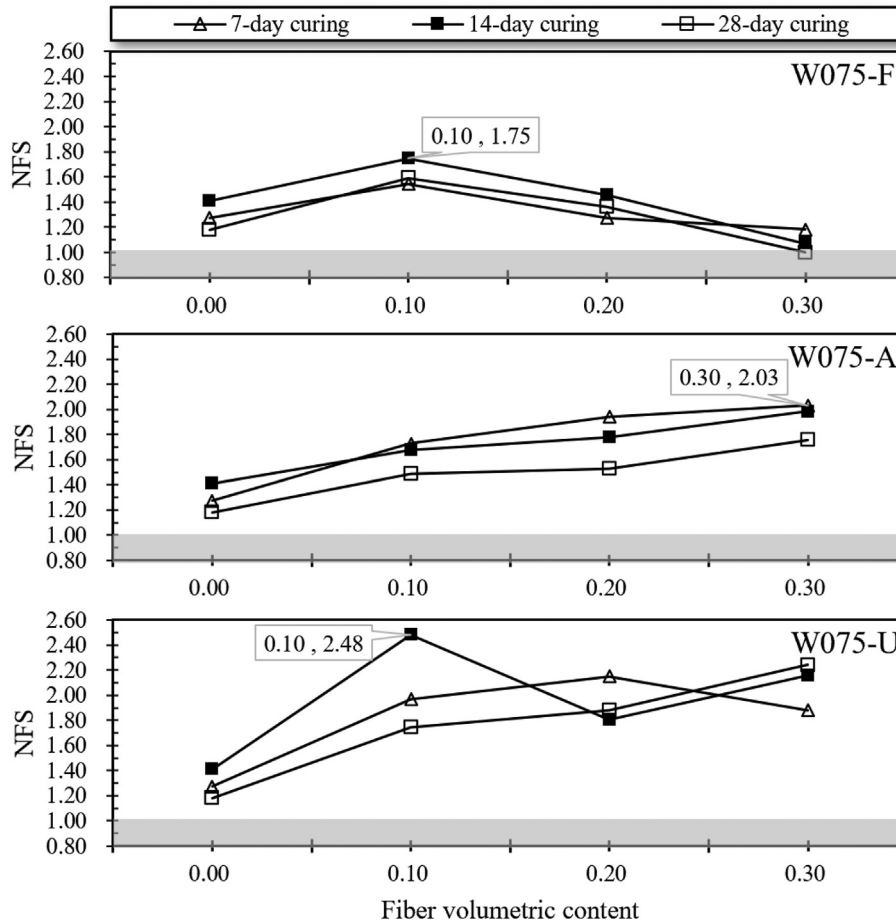


Fig. 13 – Flexural strength enhancement for W075 group.

performance only for specimens mixed with wollastonite pozzolan with adequate curing time.

3.4. Statistics of optimal combination of design variables

The rankings of NFS and NCS enhancement performance with different combinations of pozzolan type, fiber volumetric content, fiber treatment method and curing time are presented in Tables 5 and 6, respectively. Use of the above rankings is able to provide guidance in design of SCC mixtures aiming to achieve the optimization of mechanical performance and material consumption.

It is found that the best strength enhancement of both NFS and NCS comes from the same variable combination, i.e., the W-075 specimen reinforced by the fiber under treatment of UVCT with 0.1 volumetric content and under 14-day curing time. It is also noteworthy that the treatment of UVCT on fibers tends to provide the maximum strength enhancement more easily than the other two treatments, as shown in Table 6, 80 percent of specimens with the maximum NCS enhancement performance constitute UVCT on different fibers.

Additionally, it is observed that longer curing time tends to provide the maximum NFS enhancement more easily, as

evidenced in Table 5 by five specimens for 14- and 28-day curing time, respectively, while two specimens for 7-day curing time. However, the curing time manifests an opposite impact on NCS enhancement performance, as evidenced by the lower rankings of specimens with 28-day curing time in Table 6. Moreover, the rankings indicate that the specimens reinforced by W-075 fiber provide a prominent strength enhancement performance than other types of fibers for both NFS and NCS.

It should also be noted that the increasing fiber volumetric content could not lead to the increasing strength enhancement performance. Over 66% of specimens with the maximum NCS and NFS enhancement performance for different fiber types were reinforced with fiber volumetric content lower than 0.1%. Accordingly, as derived in the above statistical analysis, the specimens with pozzolan of W-075, and/or the fiber treatment of UVCT, and/or the low fiber volumetric content (e.g., 0.1) tend to develop the maximum strength enhancement than those with other variable levels.

3.5. Variable significance analysis

According to the sensitivity analysis, the variable importance can be ranked as shown in Table 7. The curing time is the most important variable for both compressive strength and flexural

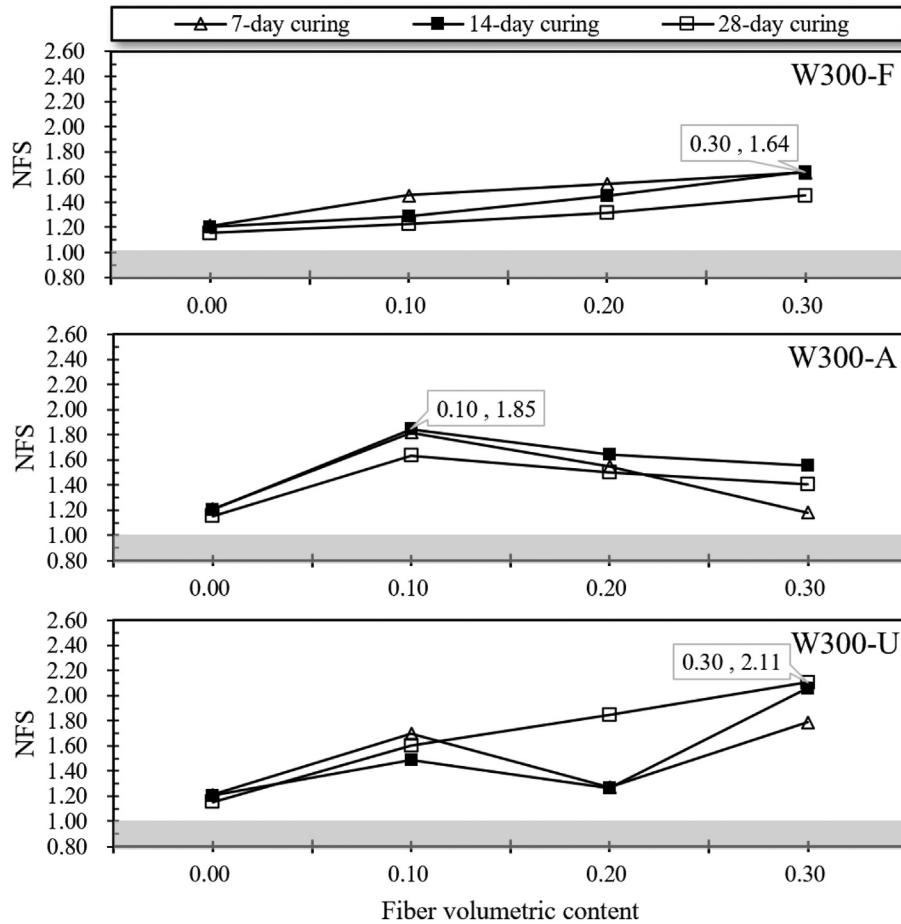


Fig. 14 – Flexural strength enhancement for W300 group.

strength. Besides, the size of zeolite and wollastonite is relatively more important in regard to compressive strength than to flexural strength. It is noted that the Jute fiber treatments (i.e. UVCT, AAT) are significant especially on flexural strength. Compared to AAT, the UVCT presented higher importance on SCC mechanical properties.

3.6. Microstructural interpretation

Aiming to investigate the mechanism of the fiber treatment methods, the microstructure morphology of the fracture surfaces of different SCC specimens was captured after the flexural strength test.

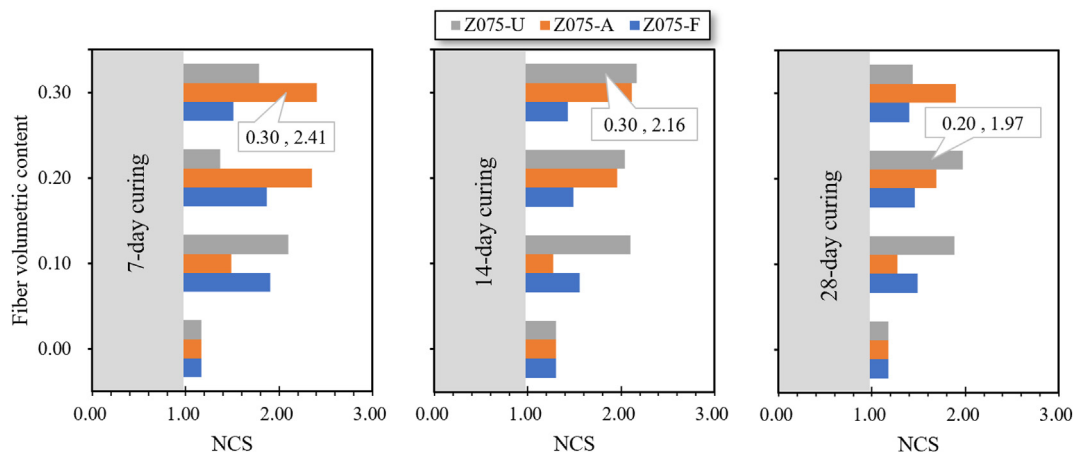


Fig. 15 – Compressive strength enhancement for Z075 group.

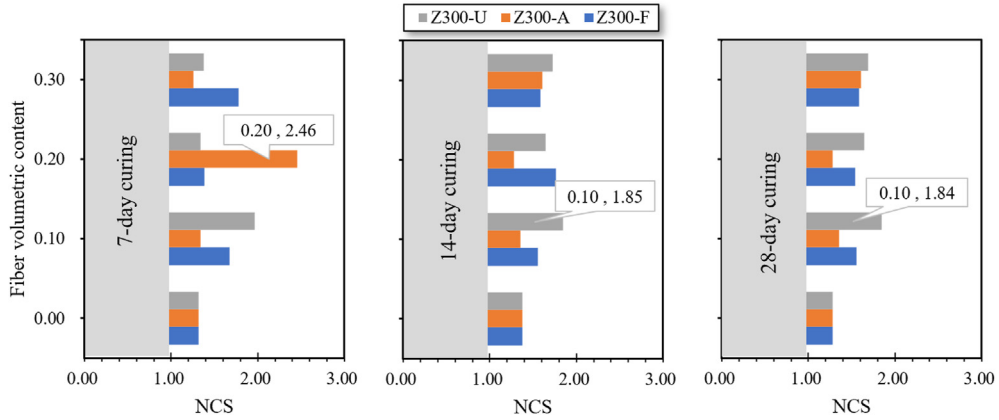


Fig. 16 – Compressive strength enhancement for Z300 group.

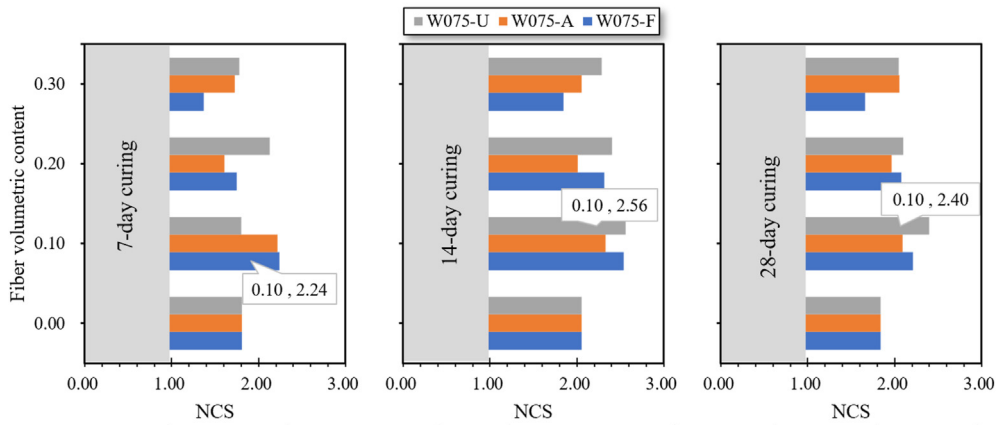


Fig. 17 – Compressive strength enhancement for W075 group.

The microstructure morphology of the three types of jute fiber specimens were captured using SEM as shown in Fig. 19. It is obviously observed in Fig. 19b that the fiber under AAT experienced the cross-sectional shrinkage and manifested

with lower moisture condition. The coating effectiveness of fiber under UVCT can be evidenced in Fig. 19c by the presence of silica layer around the surficial periphery of fiber. Both treatment methods could improve the surface microstructure

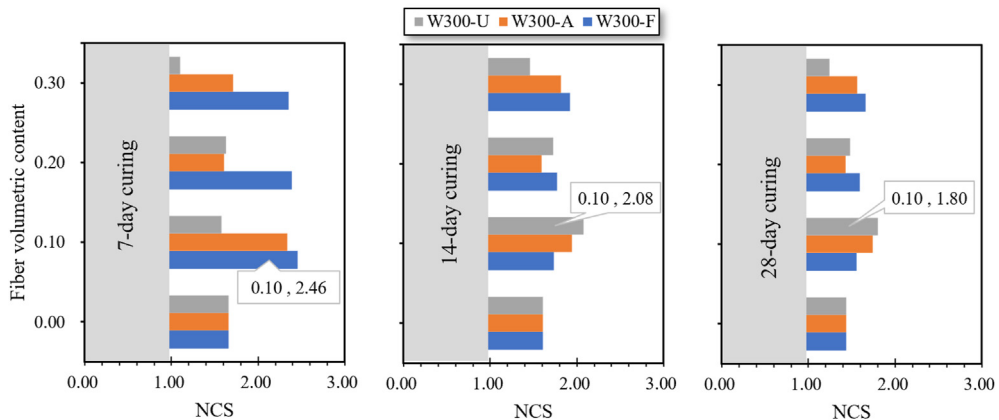


Fig. 18 – Compressive strength enhancement for W300 group.

Table 5 – Testing variable combinations corresponding to the maximum NFS for different fibre inclusions.

Sample type	Fiber content (vol%)	Curing time (day)	Fibre treatment	NFS (MPa)	Rankings
Z-075	0	14	F	1.49	12
	0.1	28	A	1.95	5
	0.2	28	U	1.92	6
Z-300	0	28	F	1.55	11
	0	28	A	1.55	10
	0.2	7	U	2.42	2
W-075	0.1	14	F	1.75	8
	0.3	7	A	2.03	4
	0.1	14	U	2.48	1
W-300	0.3	14	F	1.64	9
	0.1	14	A	1.85	7
	0.3	28	U	2.11	3

Table 6 – Testing variable combinations corresponding to the maximum NCS for different fibre inclusions.

Sample type	Fiber content (vol%)	Curing time (day)	Fibre treatment	NCS (MPa)	Rankings
Z-075	0.3	7	A	2.41	4
	0.3	14	U	2.16	7
	0.2	28	U	1.97	9
Z-300	0.2	7	A	2.46	3
	0.1	14	U	1.85	10
	0.1	28	U	1.84	11
W-075	0.1	7	F	2.24	6
	0.1	14	U	2.56	1
	0.1	28	U	2.4	5
W-300	0.1	7	F	2.46	2
	0.1	14	U	2.08	8
	0.1	28	U	1.8	12

of jute fiber, which may finally enhance the bonding behaviors between the jute fiber and cement matrix. The feasibility and effectiveness of these treatment methods will be furtherly discussed based on the mechanical properties and microstructure analysis.

The microstructures of fracture surfaces after mechanical tests were also observed in three different modification methods, as shown in Fig. 20. The specimens containing jute fiber without proper treatment display apparent gaps at the interface between jute fiber and cement matrix. On the one hand, the free-of-treatment jute fiber has a smooth surface that may undermine the mechanical cohesion between the fiber and cement matrix. On the other hand, the original jute fiber is an organic material, while the cement matrix is an inorganic material, these two types of material cannot generate chemical bonds between them. However,

after the AAT treatment, the surface microstructure was modified, the modified jute fiber showed a crude surface when compared with that of the original fiber, which finally contributed to a better mechanical bond between the fiber and cement hydration products [57,58]. In addition, with the UVCT treatment, not only the cement hydration products can be captured on the fiber surface, but also the improved interface bonding structure was obtained.

3.7. Sustainability analysis on the greenhouse gas (GHG) emissions

To achieve the ecological concrete materials, the GHG emissions of the proposed ecological concrete were calculated and compared with normal concrete material without the addition of jute fiber and waste mineral powders. The GHG emissions during the production of cement was conducted since most GHG emission of concrete materials occurred during the cement production [59,60]. In the meanwhile, global cement production is dominated by China, which accounted for more than 58% of the total cement production in 2013 all over the world [61]. The cement production emissions dataset of China was obtained from Kajaste and Hurme [62]. In 2011, 2085 Mt cement was produced in China, which led to extremely large CO₂ emissions of 1440.74 Mt. Therefore, the specific emission of cement production was calculated as 691 kg CO₂/t. Afterwards, the specific emission of waste mineral powder was obtained based on the average value of zeolite and

Table 7 – Input variables importance evaluation for compressive and flexural strength.

Variable	Importance ratio for CS (%)	Importance ratio for FS (%)
Curing time	54.47	54.19
Pozzolan size	13.13	1.12
Wollastonite	12.05	7.48
UVCT	6.52	32.13
Zeolite	6.01	4.94
AAT	4.10	11.50
Jute fiber content	3.72	4.32

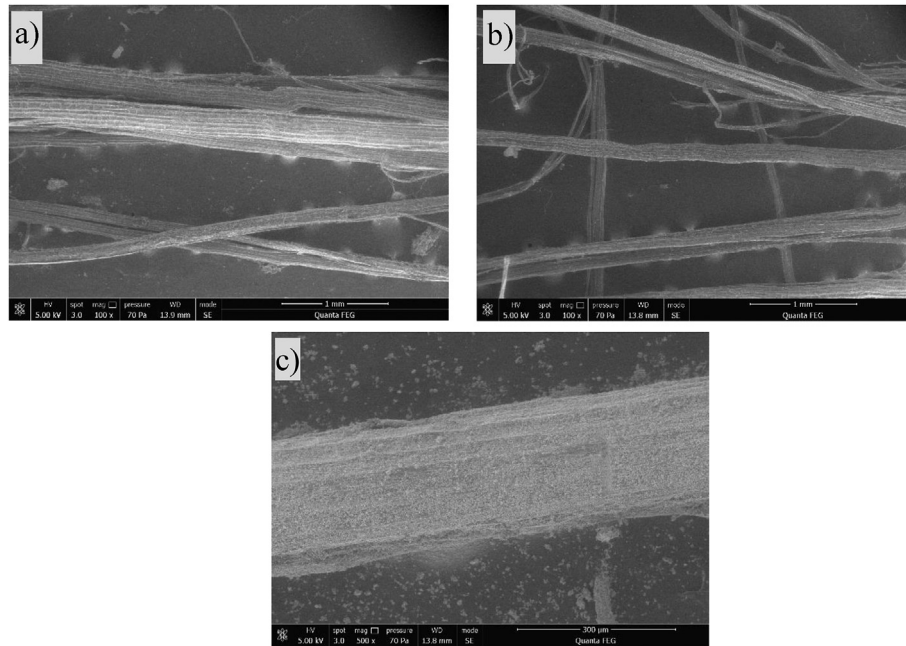


Fig. 19 – The microstructure of jute fiber: (a) FOT specimen without treatment; (b) AAT treated specimen; (c) UVCT treated specimen.

wollastonite. It has been computed based on the research of Worathanakul et al. [63] and Nair et al. [64] as 14.84 kg CO₂/t. In addition, the production processes of jute fiber account for about 320 kg CO₂/t. The datasets are summarized as shown in Table 8.

For a comparative study, the conventional SCC mixture with an only cement binder and ecological jute fiber

reinforced SCC mixture with waste mineral powders was calculated based on the consistent volume of 1 m³. After replacing the 15% cement with waste mineral powder and adding 1% jute fiber based on the recommended compositions from the experimental test results, the CO₂ emission was significantly reduced by 14.2%. Thus, the proposed jute fiber-reinforced ecological SCC concrete material with waste

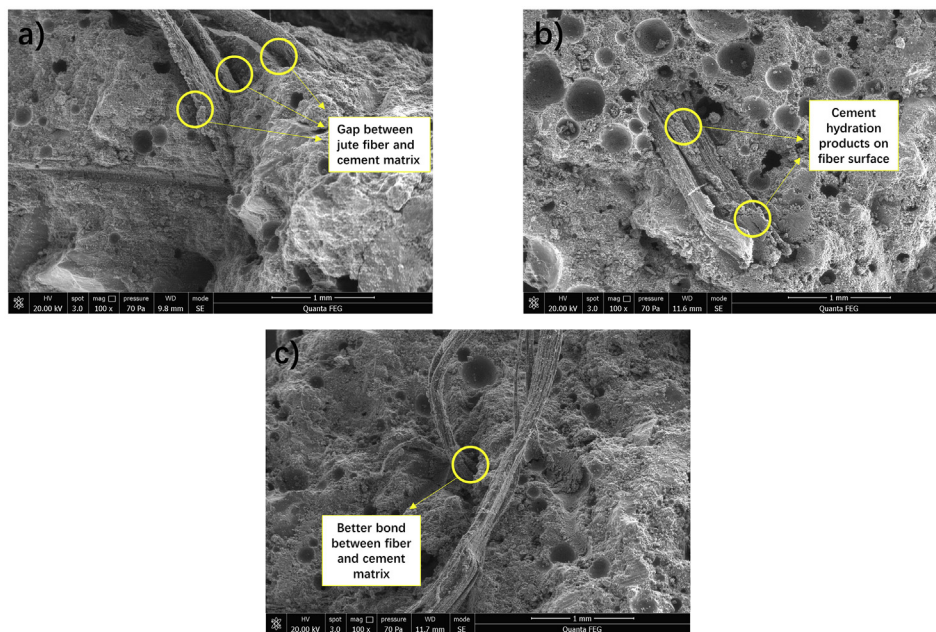


Fig. 20 – The microstructure observations on fracture surfaces of tested SCC specimens: (a) FOT specimen without treatment; (b) AAT treated specimen; (c) UVCT treated specimen.

Table 8 – The specific CO₂ emissions in different SCC mixture compositions.

Compared compositions of SCC	Specific GHG emissions (kg CO ₂ /t)
Cement	691
Waste mineral powder	14.84
Jute fiber	320

mineral powders could effectively decrease the GHG emission by reducing the cement usage, while achieving good mechanical properties for potential applications.

4. Summary and conclusions

This work presented an experimental investigation on the mechanical performance evolution of ecological jute fiber-reinforced self-compacting concrete (SCC) with minerals additives as alternative cementitious materials. The experimental results represented that the success of combining natural jute fiber and waste mineral disposals for enhancing the SCC materials as well as reducing the CO₂ emissions and cost. There are some conclusions that can be summarized below:

- (1) The flowability of jute fiber reinforced SCC mixtures with mineral powders can meet the requirement for most applications. The modification methods for jute fibers can effectively improve the fresh property of SCC mixtures in terms of the slump flow, especially the ultrasonic vibration coating treatment (UVCT) method.
- (2) The cost-effectiveness would be significantly improved with the addition of natural material and waste disposals instead of Portland cement. The introduction of jute fiber and mineral powders in SCC mixtures enhanced the mechanical performance. The addition of mineral powders can slightly improve the flexural and compressive strength, in which the smaller particle size represented more effectiveness.
- (3) Based on the statistics of optimal combination of design variables, the 0.1% fiber addition ratio with UVCT treatment method and zeolite-75mm mineral powder represented the best positive coupling effect for enhancing the mechanical properties of SCC samples. The optimized mixture design of ecological jute fiber-reinforced SCC with added pozzolans could contribute to a better sustainability with improved properties by comparing with conventional SCC materials.
- (4) The observations on the microstructure morphology of fractured SCC specimens demonstrated the mechanisms of different treatment methods. The alkali activation treatment (AAT) methods could generate a crude surface, thus improving the mechanical bond between fiber and cement matrix. With the UVCT treatment, the coated nano-sized silica layer on the jute fiber surface could participate in the cement hydration process and finally contribute to the chemical bond between the fiber and cement matrix.

- (5) The positive coupling effect of the jute fiber and mineral powder on improving the mechanical properties of SCC was verified from this investigation. The jute fiber-reinforced SCC mixes with mineral additives would become an ecological construction material with lower CO₂ emissions that is 14.2% lower than conventional SCC mixture. The environmental issues related to Portland cement production, as well as landfills related to waste mineral powders and jute could also be relieved with the application of this sustainable material.

Declaration of Competing Interest

The authors declare that they have no known competing financial interests or personal relationships that could have appeared to influence the work reported in this paper.

Acknowledgments

This research was sponsored by the National Natural Science Foundation of China (grant numbers 51978254 and 51908201), Natural Science Foundation of Hunan Province (grant number 2020JJ5024) and Academic Research Council of Australia Linkage Projects for Asset Intelligence: Maximising Operational Effectiveness for Digital Era, (Grant No. LP180100222). This study was supported by the National Natural Science Foundation of China (5210081716) and Natural Science Foundation of Jiangsu Province (BK20210617). This study was supported by State Key Laboratory for GeoMechanics and Deep Underground Engineering, China University of Mining & Technology/China University of Mining & Technology, Beijing (SKLGDUEK2105). The authors would like to appreciate the support by the Jiangsu 2020 Students' innovation and entrepreneurship training program (202011276014Z) and 2021 Students' innovation and entrepreneurship training program (202111276019Z, 202111276020Z).

REFERENCES

- [1] Xi F, Davis SJ, Ciais P, Crawford-Brown D, Guan D, Pade C, et al. Substantial global carbon uptake by cement carbonation. *Nat Geosci* 2016;9(12):880–3.
- [2] Pierrehumbert R. There is no Plan B for dealing with the climate crisis. *Bull At Sci* 2019;75(5):215–21.
- [3] Zhang J, Ma G, Huang Y, Aslani F, Nener B. Modelling uniaxial compressive strength of lightweight self-compacting concrete using random forest regression. *Construct Build Mater* 2019;210:713–9.
- [4] Zhang W, Li H, Wu C, Li Y, Liu Z, Liu H. Soft computing approach for prediction of surface settlement induced by earth pressure balance shield tunneling. *Undergr Space* 2021;6(4):353–63.
- [5] Siddique R. *Self-compacting concrete: materials, properties and applications*. Woodhead Publishing; 2019.
- [6] Sun J, Aslani F, Lu J, Wang L, Huang Y, Ma G. Fibre-reinforced lightweight engineered cementitious composites for 3D concrete printing. *Ceram Int* 2021;47(19):27107–21.
- [7] Sun J, Huang Y, Aslani F, Wang X, Ma G. Mechanical enhancement for EMW-absorbing cementitious material using 3D concrete printing. *J Build Eng* 2021:102763.

- [8] Sharma SK. Properties of SCC containing pozzolans, Wollastonite micro fiber, and recycled aggregates. *Heliyon* 2019;5(8):e02081.
- [9] Sun J, Aslani F, Wei J, Wang X. Electromagnetic absorption of copper fiber oriented composite using 3D printing. *Construct Build Mater* 2021;300:124026.
- [10] Feng J, Chen B, Sun W, Wang Y. Microbial induced calcium carbonate precipitation study using *Bacillus subtilis* with application to self-healing concrete preparation and characterization. *Construct Build Mater* 2021;280:122460. <https://doi.org/10.1016/j.conbuildmat.2021.122460>.
- [11] Sakai K, Noguchi T. *The sustainable use of concrete*. CRC Press; 2012.
- [12] Chen C, Habert G, Bouzidi Y, Jullien A, Ventura A. LCA allocation procedure used as an incitative method for waste recycling: an application to mineral additions in concrete. *Resour Conserv Recycl* 2010;54(12):1231–40.
- [13] Wang B, Liu L, Wang Y, Li L. Stability evaluation of reinforced concrete structure of large coastal buildings. *J Coast Res* 2020;103(SI):407–11. <https://doi.org/10.2112/SI103-083.1>.
- [14] Ye J, Huang H, Liang W, Li H. The optimization design of the geometric adaptability of the console in the medical emergency room of ship cabin based on ergonomics. *J Coast Res* 2020;103(SI):887–91. <https://doi.org/10.2112/SI103-184.1>.
- [15] Samimi K, Kamali-Bernard S, Maghsoudi AA, Lgcgm S, Civil E. Resistance to chloride penetration of high strength self-compacting concretes: pumice and zeolite effect. *Int J Civ Environ Eng* 2018;12(3):250–9.
- [16] Jindal A, Ransinchung G, Kumar P. Behavioral study of self-compacting concrete with wollastonite microfiber as part replacement of sand for pavement quality concrete (PQC). *International Journal of Transportation Science and Technology* 2020;9(2):170–81.
- [17] Florea M, Brouwers H. Chloride binding related to hydration products: Part I: ordinary Portland Cement. *Cement Concr Res* 2012;42(2):282–90.
- [18] Sun J, Wang Y, Liu S, Dehghani A, Xiang X, Wei J, et al. Mechanical, chemical and hydrothermal activation for waste glass reinforced cement. *Construct Build Mater* 2021;301:124361.
- [19] Aslani F, Sun J, Bromley D, Ma G. Fiber-reinforced lightweight self-compacting concrete incorporating scoria aggregates at elevated temperatures. *Struct Concr* 2019;20(3):1022–35.
- [20] Wang M, Yang X, Wang W. Establishing a 3D aggregates database from X-ray CT scans of bulk concrete. *Construct Build Mater* 2022;315:125740. <https://doi.org/10.1016/j.conbuildmat.2021.125740>.
- [21] Liu W, Guo Z, Wang C, Niu S. Physico-mechanical and microstructure properties of cemented coal Gangue-Fly ash backfill: effects of curing temperature. *Construct Build Mater* 2021;299:124011. <https://doi.org/10.1016/j.conbuildmat.2021.124011>.
- [22] Zhang G, Chen C, Li K, Xiao F, Sun J, Wang Y, et al. Multi-objective optimisation design for GFRP tendon reinforced cemented soil. *Construct Build Mater* 2022;320:126297.
- [23] Feng W, Wang Y, Sun J, Tang Y, Wu D, Jiang Z, et al. Prediction of thermo-mechanical properties of rubber-modified recycled aggregate concrete. *Construct Build Mater* 2022;318:125970.
- [24] Zhang W, Tang Z. Numerical modeling of response of CFRP–Concrete interfaces subjected to fatigue loading. *J Compos Construct* 2021;25(5). [https://doi.org/10.1061/\(ASCE\)CC.1943-5614.0001154.04021043](https://doi.org/10.1061/(ASCE)CC.1943-5614.0001154.04021043).
- [25] Aslani F, Hou L, Nejadi S, Sun J, Abbasi S. Experimental analysis of fiber-reinforced recycled aggregate self-compacting concrete using waste recycled concrete aggregates, polypropylene, and steel fibers. *Struct Concr* 2019;20(5):1670–83.
- [26] Lu N, Wang H, Wang K, Liu Y. Maximum probabilistic and dynamic traffic load effects on short-to-medium span bridges. *Comput Model Eng Sci* 2021;127(1):345–60. <https://doi.org/10.32604/cmescs.2021.013792>.
- [27] Ramli M, Kwan WH, Abas NF. Strength and durability of coconut-fiber-reinforced concrete in aggressive environments. *Construct Build Mater* 2013;38:554–66.
- [28] Tang Y, Feng W, Chen Z, Nong Y, Guan S, Sun J. Fracture behavior of a sustainable material: recycled concrete with waste crumb rubber subjected to elevated temperatures. *J Clean Prod* 2021:128553.
- [29] Luo Y, Zheng H, Zhang H, Liu Y. Fatigue reliability evaluation of aging prestressed concrete bridge accounting for stochastic traffic loading and resistance degradation. *Adv Struct Eng* 2021;24(13):3021–9. <https://doi.org/10.1177/13694332211017995>.
- [30] Zhao R, Zhang L, Guo B, Chen Y, Fan G, Jin Z, et al. Unveiling substitution preference of chromium ions in sulphoaluminate cement clinker phases. *Compos B Eng* 2021;222:109092. <https://doi.org/10.1016/j.compositesb.2021.109092>.
- [31] Wang J, Zhang J, Feng P. Effects of tool vibration on fiber fracture in rotary ultrasonic machining of C/SiC ceramic matrix composites. *Compos B Eng* 2017;129:233–42.
- [32] Li S, Zhang X, Ding Z. The impact of public participation on the environmental impact assessment of marine engineering. *J Coast Res* 2020;103(SI):479–83. <https://doi.org/10.2112/SI103-097.1>.
- [33] Sheng C, He G, Hu Z, Chou C, Shi J, Li J, et al. Yarn on yarn abrasion failure mechanism of ultrahigh molecular weight polyethylene fiber. *Journal of Engineered Fibers and Fabrics* 2021;16. <https://doi.org/10.1177/15589250211052766>. 15589250211052766.
- [34] Aslani F, Sun J, Huang G. Mechanical behavior of fiber-reinforced self-compacting rubberized concrete exposed to elevated temperatures. *J Mater Civ Eng* 2019;31(12). 04019302.
- [35] Huang H, Huang M, Zhang W, Yang S. Experimental study of predamaged columns strengthened by HPFL and BSP under combined load cases. *Structure and infrastructure engineering* 2021;17(9):1210–27. <https://doi.org/10.1080/15732479.2020.1801768>.
- [36] Zhang R, Wu C, Goh AT, Böhlke T, Zhang W. Estimation of diaphragm wall deflections for deep braced excavation in anisotropic clays using ensemble learning. *Geosci Front* 2021;12(1):365–73.
- [37] Sun J, Lin S, Zhang G, Sun Y, Zhang J, Chen C, et al. The effect of graphite and slag on electrical and mechanical properties of electrically conductive cementitious composites. *Construct Build Mater* 2021;281:122606.
- [38] Sun J, Ma Y, Li J, Zhang J, Ren Z, Wang X. Machine learning-aided design and prediction of cementitious composites containing graphite and slag powder. *J Build Eng* 2021:102544.
- [39] Li J, Qin Q, Sun J, Ma Y, Li Q. Mechanical and conductive performance of electrically conductive cementitious composite using graphite, steel slag, and GGBS. *Structural Concrete*; 2020.
- [40] Zhang C, Abedini M. Development of PI model for FRP composite retrofitted RC columns subjected to high strain rate loads using LBE function. *Eng Struct* 2022;252:113580. <https://doi.org/10.1016/j.engstruct.2021.113580>.
- [41] Wang D, Ju Y, Shen H, Xu L. Mechanical properties of high performance concrete reinforced with basalt fiber and polypropylene fiber. *Construct Build Mater* 2019;197:464–73. <https://doi.org/10.1016/j.conbuildmat.2018.11.181>.

- [42] Sun J, Huang Y, Aslani F, Ma G. Properties of a double-layer EMW-absorbing structure containing a graded nano-sized absorbent combing extruded and sprayed 3D printing. *Construct Build Mater* 2020;261:120031.
- [43] Standards Australia Sydney. AS1012.9 methods of testing concrete: compressive strength tests-concrete, mortar and grout specimens. 2014.
- [44] Zhang W, Li H, Li Y, Liu H, Ding X. Application of deep learning algorithms in geotechnical engineering: a short critical review. *Artif Intell Rev* 2021;(9):1–41.
- [45] Zhang W, Wu C, Zhong H, Li Y, Wang L. Prediction of undrained shear strength using extreme gradient boosting and random forest based on Bayesian optimization. *Geosci Front* 2021;12(1):469–77.
- [46] EFNARC. Specifications and guidelines for self-compacting concrete. UK: EFNARC; 2005.
- [47] AS1012.14 methods of testing concrete method 14: method for securing and testing cores from hardened concrete for compressive strength. *Materials tests*; 1991.
- [48] C348 A. ASTM Standard test method for flexural strength of hydraulic-cement mortars. West Conshohocken, Pennsylvania, United States: American Society for Testing and Materials International; 2008.
- [49] Cortez P, Embrechts MJ. Opening black box data mining models using sensitivity analysis. In: 2011 IEEE symposium on computational intelligence and data mining (CIDM). IEEE; 2011.
- [50] Cortez P, Embrechts MJ. Using sensitivity analysis and visualization techniques to open black box data mining models. *Inf Sci* 2013;225:1–17. <https://doi.org/10.1016/j.ins.2012.10.039>.
- [51] Ning F, He G, Sheng C, He H, Wang J, Zhou R, et al. Yarn on yarn abrasion performance of high modulus polyethylene fiber improved by graphene/polyurethane composites coating. *Journal of Engineered Fibers and Fabrics* 2021;16. <https://doi.org/10.1177/1558925020983563>. 1558925020983563.
- [52] Sun J, Wang J, Zhu Z, He R, Peng C, Zhang C, et al. Mechanical performance prediction for sustainable high-strength concrete using bio-inspired neural network. *Buildings* 2022;12(1):65.
- [53] Xu J, Wu Z, Chen H, Shao L, Zhou X, Wang S. Study on strength behavior of basalt fiber-reinforced loess by digital image technology (DIT) and scanning electron microscope (SEM). *Arabian J Sci Eng* 2021;46(11):11319–38. <https://doi.org/10.1007/s13369-021-05787-1>.
- [54] Wang J, Dai Q, Si R, Guo S. Mechanical, durability, and microstructural properties of macro synthetic polypropylene (PP) fiber-reinforced rubber concrete. *J Clean Prod* 2019;234:1351–64.
- [55] Sun J, Tang Y, Wang J, Wang X, Wang J, Yu Z, et al. A multi-objective optimisation approach for activity excitation of waste glass mortar. *J Mater Res Technol* 2022;17:2280–304.
- [56] Sun J, Wang X, Zhang J, Xiao F, Sun Y, Ren Z, et al. Multi-objective optimisation of a graphite-slag conductive composite applying a BAS-SVR based model. *J Build Eng* 2021;44:103223.
- [57] Wang J, Dai Q, Si R. Experimental and numerical investigation of fracture behaviors of steel fiber-reinforced rubber self-compacting concrete. *J Mater Civ Eng* 2022;34(1). 04021379.
- [58] Wang J, Dai Q, Si R, Guo S. Investigation of properties and performances of Polyvinyl Alcohol (PVA) fiber-reinforced rubber concrete. *Construct Build Mater* 2018;193:631–42.
- [59] Ma W, Wang X, Wang J, Xiang X, Sun J. Generative design in building information modelling (BIM): approaches and requirements. *Sensors* 2021;21(16):5439.
- [60] Zhang W, Zhang R, Wu C, Goh ATC, Lacasse S, Liu Z, et al. State-of-the-art review of soft computing applications in underground excavations. *Geosci Front* 2020;11(4):1095–106.
- [61] Wang T, Wang J, Wu P, Wang J, He Q, Wang X. Estimating the environmental costs and benefits of demolition waste using life cycle assessment and willingness-to-pay: a case study in Shenzhen. *J Clean Prod* 2018;172:14–26.
- [62] Kajaste R, Hurme M. Cement industry greenhouse gas emissions—management options and abatement cost. *J Clean Prod* 2016;112:4041–52.
- [63] Worathanakul P, Tobaramееkul P. Development of NaY zeolite derived from biomass and environmental assessment of carbon dioxide reduction. In: MATEC web of conferences. EDP Sciences; 2016.
- [64] Nair NA, Sairam V. Research initiatives on the influence of wollastonite in cement-based construction material-A review. *J Clean Prod* 2020:124665.